Chinese Journal of Polymer Science Vol. 32, No. 3, (2014), 255–267

Chinese Journal of Polymer Science
© Chinese Chemical Society
Institute of Chemistry, CAS
Springer-Verlag Berlin Heidelberg 2014

Studies on Droplet Size Distributions during Coalescence in Immiscible Polymer Blends Filled with Silica Nanoparticles*

Zhi-ming Zou, Zhao-yan Sun** and Li-jia An
State Key Laboratory of Polymer Physics and Chemistry, Changchun Institute of Applied Chemistry, Chinese Academy of Sciences, Changchun 130022, China

Abstract The effect of silica nanoparticles on the morphology of (10/90 wt%) PDMS/PBD blends during the shear induced coalescence of droplets of the minor phase at low shear rate was investigated systematically *in situ* by using an optical shear technique. Two blending procedures were used: silica nanoparticles were introduced to the blends by pre-blending silica particles first in PDMS dispersed phase (procedure 1) or in PBD matrix phase (procedure 2). Bimodal or unimodal droplet size distributions were observed for the filled blends during coalescence, which depend not so much on the surface characteristics of silica but mainly on blending procedure. For pure (10/90 wt%) PDMS/PBD blend, the droplet size distribution exhibits bimodality during the early coalescence. When silica nanoparticles (hydrophobic and hydrophilic) were added to the blends with procedure 1, bimodal droplet size distributions disappear and unimodal droplet size distributions can be maintained during coalescence; the shape of the different peaks is invariably Gaussian. Simultaneously, coalescence of the PDMS droplets was suppressed efficiently by the silica nanoparticles. It was proposed that with this blending procedure the nanoparticles should be mainly kinetically trapped at the interface or in the PDMS dispersed phase, which provides an efficient steric barrier against coalescence of the PDMS dispersed phase. However, bimodal droplet size distributions in the early stage of coalescence still occur when incorporating silica nanoparticles into the blends with procedure 2, and then coalescence of the PDMS droplets cannot be suppressed efficiently by the silica nanoparticles. It was proposed that with this blending protocol the nanoparticles should be mainly located in the PBD matrix phase, which leads to an inefficient steric barrier against coalescence of the PDMS dispersed phase; thus the morphology evolution in these filled blends is similar to that in pure blend and bimodal droplet size distributions can be observed during the early coalescence. These results imply that exploiting non-equilibrium processes by varying preparation protocol may provide an elegant route to regulate the temporal morphology of the filled blends during coalescence.

Keyword: Droplet size distribution; Immiscible polymer blends; Coalescence; Silica nanoparticles.

INTRODUCTION

The temporal development of the size of droplets and their size distribution in mechanical fields is of prime importance for every production process involving immiscible polymeric blends. However, due to the complex interplay between coalescence and break-up during processing, it is extremely difficult to control the morphology of immiscible polymer blends. To achieve fine phase morphology during the processing of immiscible polymer blends, one of the classical methods is the addition of conventional compatibilizers, such as block copolymers. Due to their dual chemical nature, block copolymers usually have a strong tendency to adsorb at the two-phase interface to form highly stable monolayers and suppress coalescence of the dispersed phase. However, this technique is typically not very cost-effective since block copolymers are usually made by

* This work was financially supported by the National Basic Research Program of China (973 Program, 2012CB821500), and supported by the National Natural Science Foundation of China (Nos. 21222407, 21074137 and 50930001).
** Corresponding author: Zhao-yan Sun (孙昭艳), E-mail: zysun@ciac.jl.cn
Received July 1, 2013; Revised September 1, 2013; Accepted September 5, 2013
doi: 10.1007/s10118-014-1411-3

chemically sophisticated synthetic routes and are specific for polymer pairs.

In recent years, a new concept of "particulate compatibilizers" by using solid particles has been introduced. As discussed by Aveyard *et al*.[1] particles can be trapped irreversibly at interfaces by the effects of interfacial tension and can sometimes have effects that are similar to conventional block copolymer compatibilizers. Actually, this area of research has been stimulated by similar research in particle-stabilized oil/water emulsions, commonly described as "Pickering emulsions"[2]. Since the pioneer works of Ramsden[3] and Pickering[4], extensive efforts have been dedicated to the stability of oil/water emulsions by incorporating solid particles[5–12]. It is found that the effectiveness of particles in stabilizing an emulsion depends on several fundamental parameters such as their size, wettability, their initial location, as well as on the level of interparticle interactions. The mechanisms by which particles stabilize against coalescence are not completely understood yet. Vignati and Piazza[13] proposed that the most probable mechanism of morphology stabilization is a steric hindrance or surface rheology effects due to the particle adsorption at the interface rather than a decrease of the interfacial tension between the two liquids.

The addition of inorganic nanoparticles to immiscible polymer blends seems to be a more 'generic' way to achieve fine phase morphology and provides additional opportunities to tailor the properties of the composite material. There have been several investigations of particles adsorbed at the interfaces in polymer blends, and their effects on the morphology and properties of those blends. Carbon black[14–18], organoclay[19–24] and silica nanoparticles[25–29] have been used in these studies. It is found that the incorporation of a few percent of the nanoparticles during melt processing of the components causes a substantial reduction of the size of the dispersed phase for those blends. These refined blend morphologies have typically been attributed to the accumulation of the fillers at the interface, which acts as physical barrier preventing the coalescence of the dispersed phase. Although the effect of nanoparticles on the morphology of immiscible polymer blends has drawn great attention recently, the investigations concerning the temporal development of the size of droplets and their size distribution during coalescence in the filled immiscible polymer blends are rather scarce. However, the temporal morphology of the blends is very central for their properties, so understanding how to regulate the temporal morphology of the blends is not only interesting from the viewpoint of fundamental polymer science but also provides an approach to the formation of special structures and morphologies for industrial polymeric materials.

It should be mentioned that due to high viscous of immiscible polymer blends, kinetic effects may play a key role and thus the localization of the nanoparticles in the blends can be affected by varying the blending procedure[30]. And we can suppose two situations for the localization of the nanoparticles if the kinetic effects dominate the mixing procedure: the nanoparticles can be expected to be mainly kinetically trapped at the interface or in the dispersed phase when incorporating them into the blends by pre-blending particles with the dispersed phase; and they can be mainly kinetically trapped in the matrix phase when incorporating them into the blends by pre-blending particles with the matrix phase. For the above two situations, different temporal morphology of the blends can be anticipated during coalescence, due to the differed location of the nanoparticles which might had a significant effect on the coalescence behavior of the dispersed phase. Thus exploiting nonequilibrium processes by changing blending procedure may provide an elegant route to regulate the temporal morphology of the filled blends during coalescence.

In this work, we first concerned how the size and distribution of the droplets of the minor phase change with time during coalescence in the absence of breakup processes in immiscible polymer blends filled with nanoparticles. For this study, we chose a blend of (10/90 wt%) PDMS/PBD as model system, and then we added silica nanoparticles into the blend. Furthermore, we explored possibilities of applying preparation protocols to regulate the temporal morphology of the filled blends during coalescence. The influences of concentration and surface characteristics (hydrophobic and hydrophilic) of silica nanoparticles on the temporal morphology of (10/90 wt%) PDMS/PBD blends were also investigated *in situ* by using an optical shear technique.

EXPERIMENTAL

Materials

Experiments were performed on an immiscible blend of polydimethylsiloxane (PDMS from Alfa Aesar, M_w = 63000) and polybutadiene (PBD from Aldrich, M_n = 3000). All experiments were done at 25 °C. At this temperature PBD and PDMS are liquid polymers, thereby avoiding thermal degradation problems typically encountered with polymer melts. Viscosities were measured with an advanced rheometric expansion system (ARES-G2) from TA Instruments Corp, USA. Within the investigated range of shear rates (0–30 s^{-1}) PBD and PDMS behave Newtonian. The interfacial tension σ is 4.1 mN/m at 25 °C. The characteristic data of the polymers are collected in Table 1. The silica content was in the range of 0.1–1.0 wt% of the total material and the proportion of PDMS in PBD was always 10 wt%.

Table 1. Densities, viscosities and refractive indexes of the polymers at 25 °C

Polymer	Density (g/mL)	Viscosity (Pa·s)	Refractive index
PBD	0.90	4.8	1.52
PDMS	0.97	10.4	1.40

Two types of nanosilica (SiO_2) were used: hydrophobic silica (Aerosil R972 with 16 nm diameter and a specific surface area of 110 ± 20 m^2/g) and hydrophilic silica (Aerosil A200 with 12 nm diameter and a specific surface area of 200 ± 25 m^2/g). Both of them were supplied by Degussa Corp.

Sample Preparation

R972 and A200 silica nanoparticles were dried before used. Blends were prepared by hand-mixing with a spatula in a small Petri-dish until a homogeneous mixture was formed and subsequently placed in a vacuum oven at room temperature to remove entrapped air bubbles. The blend of 10.0 wt% PDMS dispersed in 90.0 wt% PBD was prepared. We used two blending procedures.

Procedure 1: The nanoparticles were first mixed manually with the minor phase PDMS for ten minutes. After that, PBD was added to the resulting PDMS and an extra mixing time of 10 min was applied.

Procedure 2: The nanoparticles were first mixed manually with the matrix phase PBD for ten minutes. Then PDMS was added to the resulting PBD and an extra mixing time of 10 min was applied.

Experimental Method

All coalescence experiments were carried out using a Linkam CSS-450 shearing stage equipped with an Olympus BX-51 optical microscope at 25 °C with a gap of 500 μm. First, the mixture was pre-sheared at a high shear rate (30 s^{-1}) for 5 min to produce a homogenous dispersion with relatively narrow distribution of small droplets. Subsequently, the shear rate was lowered to 0.1 s^{-1} and the dispersed droplets were coalesced under shear flow for 720 min. In our study, we mainly focus on the change of size and distribution of the droplets for minor phase with time during coalescence in the absence of breakup processes. Therefore, a low shear rate (*i.e.*, 0.1 s^{-1}) was used to ensure that breakup of droplets cannot occur in our study. The morphology development was observed by taking digital images of the sheared sample at different times.

The droplet size was determined by image analysis. Typically, at least 200 droplets were analyzed per sample. The number average radius R_N and the volume average radius R_V were calculated based on the real particle size distribution by Eqs. (1) and (2), respectively.

$$R_N = \frac{\sum_{i=1}^{\infty} n_i R_i}{\sum_{i=1}^{\infty} n_i} \tag{1}$$

$$R_V = \frac{\sum_{i=1}^{\infty} n_i R_i^4}{\sum_{i=1}^{\infty} n_i R_i^3} \tag{2}$$

Furthermore, we determined the mean value of the Gaussian fit to the droplet size distribution R_G by Eq. (3).

$$y = y_0 + \frac{A}{SD\sqrt{2\pi}} \exp^{-((R-R_G)^2/2SD^2)} \quad (3)$$

SD: standard deviation. The size polydispersity *d* was characterized by $d = R_V/R_N$.

RESULTS AND DISCUSSION

Droplet Size Distribution-Bimodality or Unimodality

We start describing the droplet size distribution results by showing the data for the unfilled blend. The droplet size distribution exhibiting bimodality during the early stage of shear induced coalescence for (10/90 wt%) PDMS/PBD blend was observed from the image together with the obtained droplet size distribution, as shown in Fig. 1. Similar results were also reported by Wolf *et al.*[32] for poly(dimethyl-*co*-methylphenyl siloxane) /poly(dimethylsiloxane) blends and they can be interpreted in terms of collision frequencies and collision efficiencies. In other words, some of the small droplets generated after the pre-shearing step remain stable during the early stage of coalescence due to the fact that the coalescence efficiency decreases with increasing difference in the size of the coalescing droplets. It should be mentioned that, the small droplets can disappear as time advances, and the droplet size distribution can finally show unimodality. Next, we will investigate the effect of hydrophobic R972 and hydrophilic A200 silica on the droplet size distributions of (10/90 wt%) PDMS/PBD blend, respectively.

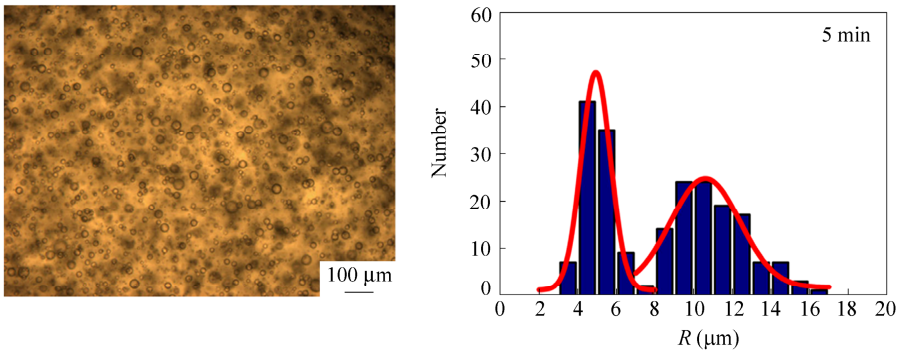


Fig. 1 Light microscopic image and droplet size distribution for the (10/90 wt%) PDMS/PBD blend at 5 min after abruptly decreasing the shear rate from 30 s^{-1} to 0.1 s^{-1} (The curves are Gaussian fits to the observed size distributions.)

Interestingly, the optical morphology and the droplet size distributions of PDMS/PBD blends with the addition of different contents of R972 nanoparticles demonstrated that bimodal droplet size distribution disappeared and unimodal droplet size distribution can be maintained during the coalescence of the dispersed phase, when the hydrophobic R972 silica was initially mixed with the dispersed phase PDMS (blending procedure 1). Typical examples are given in Fig. 2 for the PDMS/PBD blend filled with 0.2 wt% R972 silica, in terms of images and droplet size distributions. From the very beginning a very narrow droplet size distribution is observed, which shifts to higher value with progressing time. It can be fitted easily by the equation of Gauss (Eq. (3)). The droplet size distribution is always Gaussian for the R972 silica filled blends with blending procedure 1.

Experiments on the R972 silica filled blends prepared with blending procedure 2 still reveal the occurrence of bimodal droplet size distributions in the early stage of coalescence, as seen in Fig. 1 for the unfilled blend. An example for the images taken during the course of the experiments is shown in Fig. 3 together with the obtained droplet size distributions for the blend containing 0.2 wt% R972 silica with blending procedure 2. Two peaks appear in the droplet size evolution shortly after a step down of shear rate from 30 s^{-1} to 0.1 s^{-1}, while only one peak can be observed as time advances. The conditions in which bimodal droplet size distributions for the R972 silica filled blends occur in the early stage of coalescence are specified in Table 2. It is clear from the table that,

blending procedure has a decisive effect on the droplet size distribution during coalescence in the R972 silica filled blend.

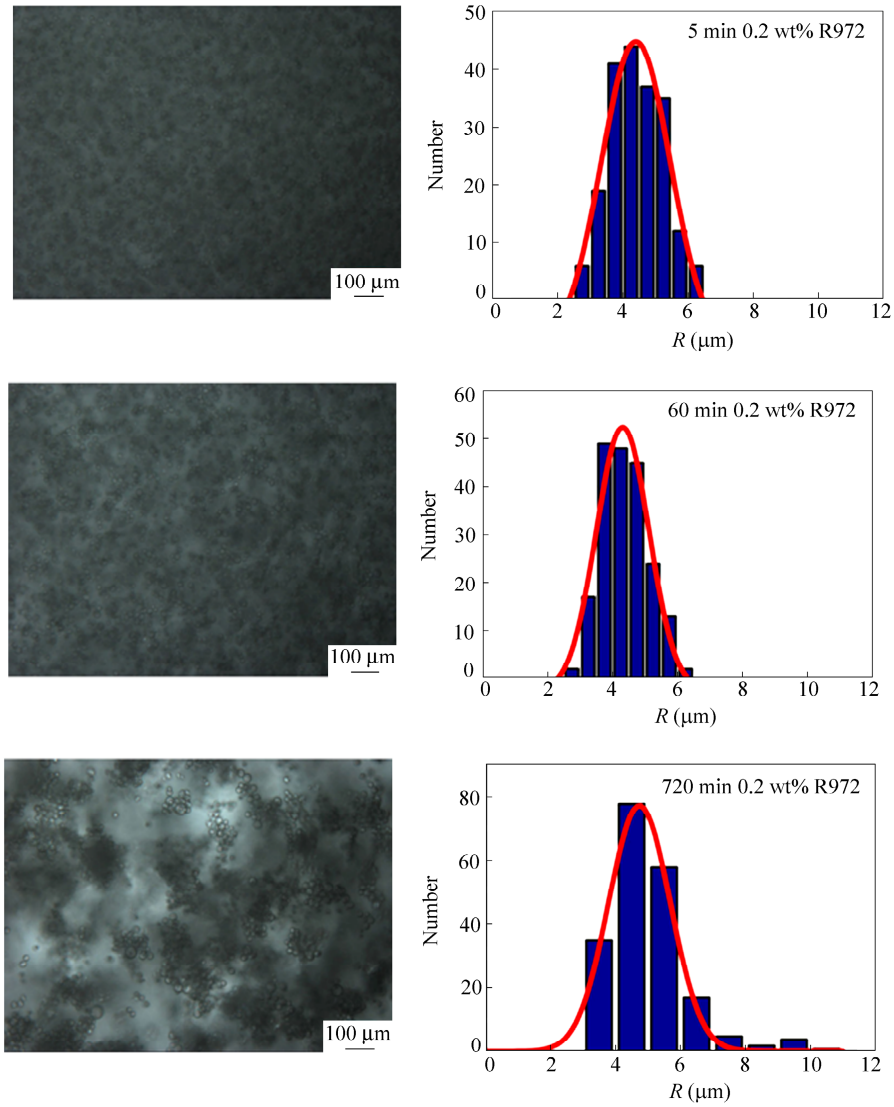


Fig. 2 Optical microscopy images and droplet size distributions for the (10/90 wt%) PDMS/PBD blend filled with 0.2 wt% R972 hydrophobic silica with blending procedure 1 at different times after abruptly decreasing the shear rate from 30 s^{-1} to 0.1 s^{-1} (The curves are Gaussian fits to the observed size distributions.)

Table 2. Influence of weight fractions of hydrophobic R972 silica filled in (10/90 wt%) PDMS/PBD blends and blending procedures on the formation of bimodal (+) or unimodal (–) droplet distributions in the early stage of coalescence

R972	0.1 wt%	0.2 wt%	0.5 wt%	1.0 wt%
Procedure 1	–	–	–	
Procedure 2	+	+	+	+

For the A200 silica filled (10/90 wt%) PDMS/PBD systems, similar results were obtained. Figure 4 shows that, with blending procedure 1, the addition of 0.2 wt% A200 silica always leads to unimodal droplet size distributions during coalescence. However, for the system still containing 0.2 wt% A200 silica but prepared with blending procedure 2, the bimodality of droplet size distribution appears again during the early stage of coalescence, as shown in Fig. 5. The conditions in which bimodal droplet size distributions for the A200 silica

filled blends occur during the early stage of coalescence are specified in Table 3. It is shown that, for the systems prepared with blending procedure 1, the droplet size distribution is always unimodal for the A200 silica filled blends except for the 0.1 wt% A200 silica filled blend.

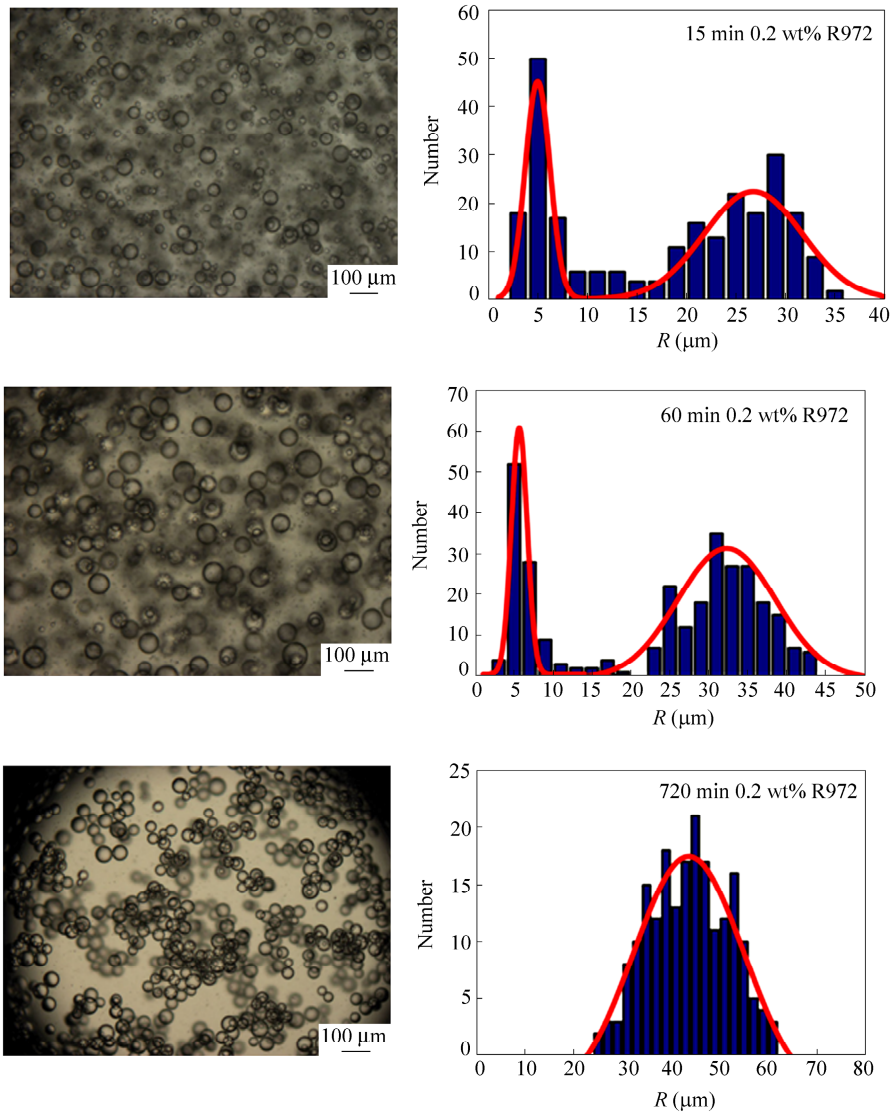


Fig. 3 Optical microscopy images and droplet size distributions for the (10/90 wt%) PDMS/PBD blend filled with 0.2 wt% R972 hydrophobic silica with blending procedure 1 at different times after abruptly decreasing the shear rate from 30 s^{-1} to 0.1 s^{-1} (The curves are Gaussian fits to the observed size distributions.)

Table 2 and Table 3 demonstrate that the droplet size distribution depends not so much on surface characteristics of silica but mainly on blending procedure. For the filled blends of (10/90 wt%) PDMS/PBD, blending procedure 1 is in favor of unimodal droplet size distribution while blending procedure 2 causes the occurrence of bimodal droplet size distribution during coalescence. From the above results, it can be concluded that, the droplet size distribution of the filled blends during coalescence can be regulated by adjusting the blending procedure. In order to further understand the influence of silica nanoparticles on the droplet size distribution, next we show how the mean droplet size evolves with time during coalescence.

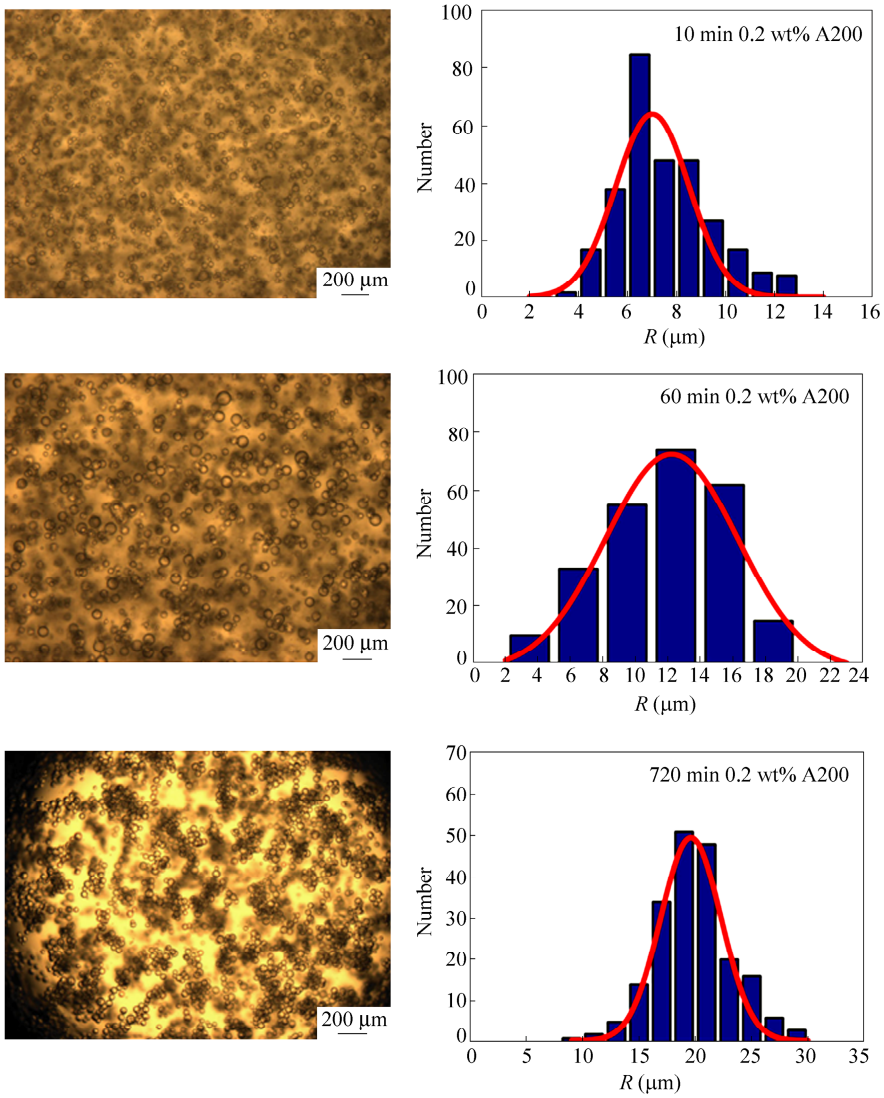


Fig. 4 Optical microscopy images and droplet size distributions for the (10/90 wt%) PDMS/PBD blend filled with 0.2 wt% A200 hydrophilic silica with blending procedure 1 at different times after abruptly decreasing the shear rate from 30 s^{-1} to 0.1 s^{-1} (The curves are Gaussian fits to the observed size distributions.)

Time Evolution of the Mean Droplet Size

Figure 6 shows how the average droplet sizes change with time during coalescence in pure (10/90 wt%) PDMS/PBD blend and R972 silica filled (10/90 wt%) PDMS/PBD blends containing different particle concentrations. It can be seen that R_V typically increases during the coalescence of the dispersed phase and the evolution of R_V clearly depends on the particle concentration and the blending procedure. Obviously, for the R972 silica filled blends, when adopting a same blending procedure, the final droplet size R_V decreases with increasing R972 silica content. The change in R_V is much smaller as compared to that of the unfilled blend, implying that coalescence is suppressed by nanoparticles. In addition, the results in Fig. 6 show that, when preparing blend with blending procedure 1, the change in R_V is much smaller than that of the filled blend containing the same particle concentration but prepared with blending procedure 2. It is implied that, for the same particle concentration, coalescence can be inhibited more effectively by particles, when preparing blend with blending procedure 1.

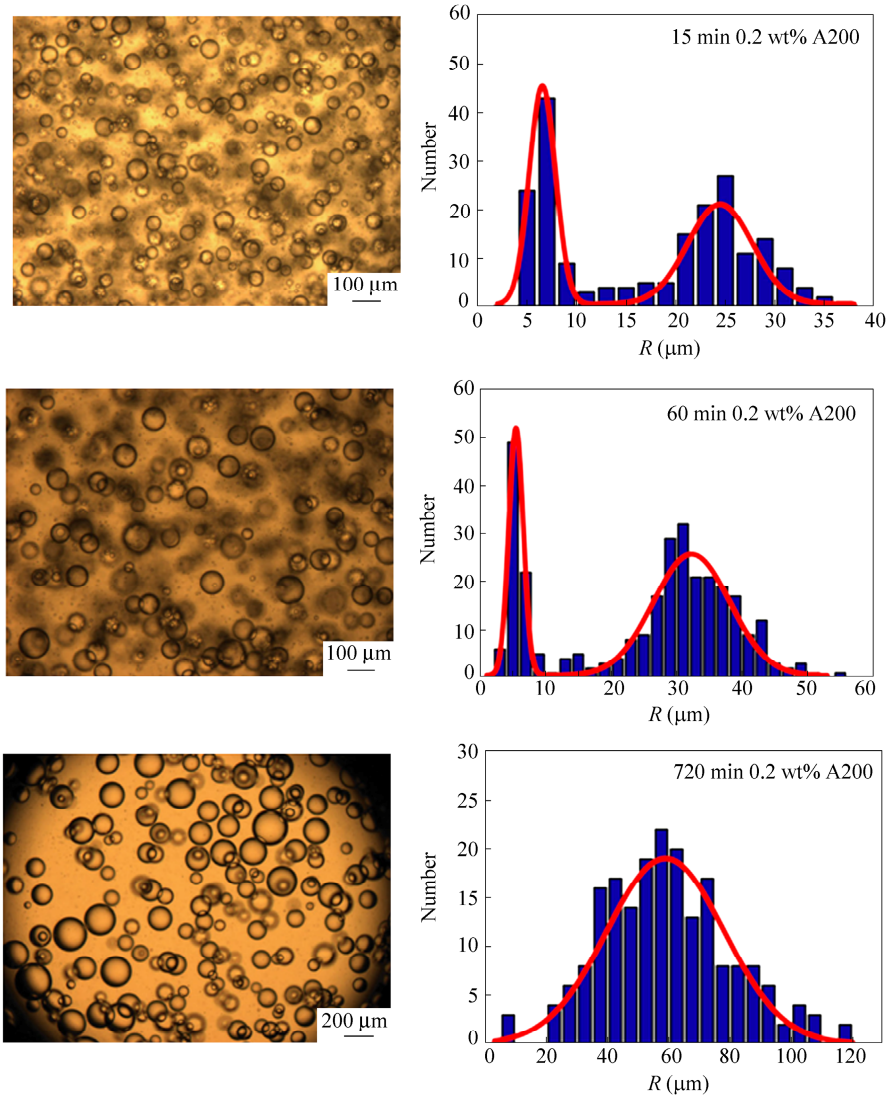


Fig. 5 Light microscopic images and droplet size distributions for the (10/90 wt%) PDMS/PBD blend filled with 0.2 wt% A200 hydrophilic silica with blending procedure 2 at different times after abruptly decreasing the shear rate from 30 s^{-1} to 0.1 s^{-1} (The curves are Gaussian fits to the observed size distributions.)

The polydispersity R_V/R_N of the droplet size as a function of time is shown in Fig. 7 for the R972 silica filled (10/90 wt%) PDMS/PBD blends. Figures 7(a) and 7(b) show the results at blending conditions of procedure 1 and 2, respectively. When preparing blend with blending procedure 2, R_V/R_N shows a maximum (approximately 1.6–1.7) for all particle concentrations in the early stage of coalescence, during the time bimodal droplet size distributions occur; however, it remains below 1.3 in all particle contents under investigation in Fig. 7(a), and the fluctuation in R_V/R_N is much smaller as compared to that in Fig. 7(b).

Table 3. Influence of weight fractions of hydrophilic A200 silica filled in (10/90 wt%) PDMS/PBD blends and blending procedures on the formation of bimodal (+) or unimodal (–) droplet distributions in the early stage of coalescence

A200	0.1 wt%	0.2 wt%	0.5 wt%	1.0 wt%
Procedure 1	+	–	–	
Procedure 2	+	+	+	+

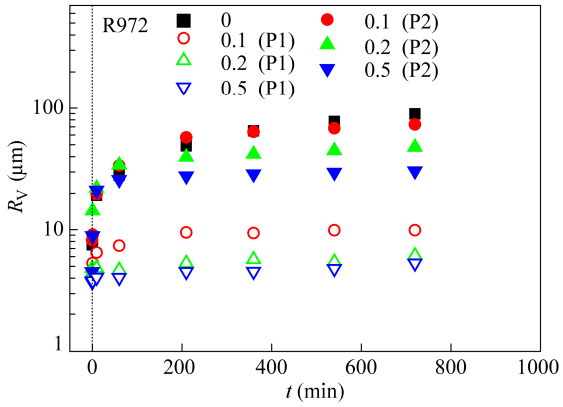


Fig. 6 Time evolution of droplet size R_V after a step down of the shear rate from 30 s^{-1} to 0.1 s^{-1} for the R972 silica filled (10/90 wt%) PDMS/PBD blends prepared with blending procedure 1 (open symbols) and with blending procedure 2 (solid symbols) (The numbers in the legend refer to particle concentrations (in wt%).)

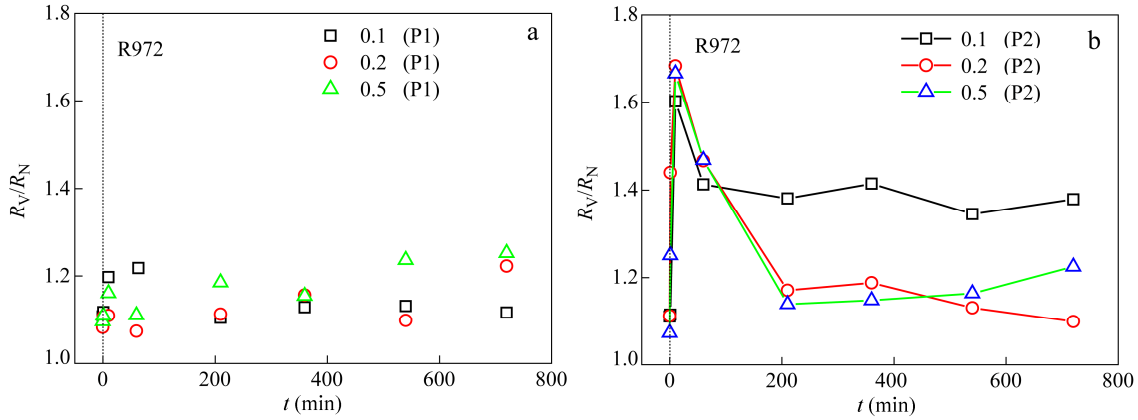


Fig. 7 Time evolution of the polydispersity of droplet radii for the R972 silica filled (10/90 wt%) PDMS/PBD blends after a step down of the shear rate from 30 s^{-1} to 0.1 s^{-1} for blends prepared (a) with blending procedure 1 and (b) with blending procedure 2 (The numbers in the legend refer to particle concentrations (in wt%).)

For the A200 silica filled (10/90 wt%) PDMS/PBD blends, the time evolution of the droplet size R_V is shown in Fig. 8. It is obvious from the figure that when preparing blend with blending procedure 1, coalescence drastically slows down for all the filled blends under investigation except for the 0.1 wt% A200 filled system. However, when preparing blend with blending procedure 2, coalescence is also suppressed but less efficient as compared to that when preparing blend with procedure 1.

Figure 9 shows how the polydispersity R_V/R_N evolves with time for A200 silica filled (10/90 wt%) PDMS/PBD systems. When preparing blend with blending procedure 2, a maximum reaches in the early stage of coalescence, as shown in Fig. 9(b), for all the A200 filled (10/90 wt%) PDMS/PBD systems. The results are similar as those shown in Fig. 7(b). When preparing blend with blending procedure 1, R_V/R_N fluctuates slightly, as shown in Fig. 9(a), for 0.2 wt% and 0.5 wt% A200 filled systems. However, it increases dramatically in the early stage of coalescence for 0.1 wt% A200 filled system.

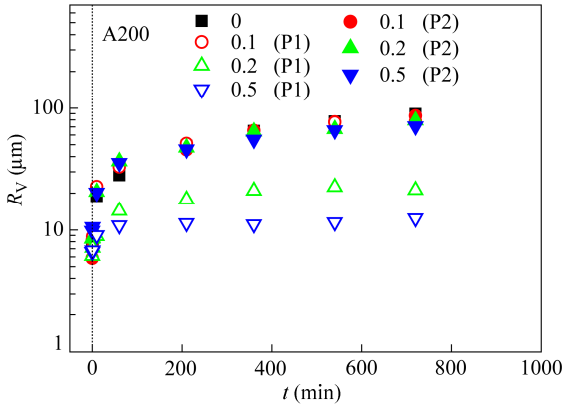


Fig. 8 R_V for the A200 silica filled (10/90 wt%) PDMS/PBD blends as a function of time after a step down of the shear rate from 30 s^{-1} to 0.1 s^{-1}
The open symbols denote the blends were prepared with blending procedure 1 and the solid ones with blending procedure 2 (The numbers in the legend refer to particle concentrations (in wt%).)

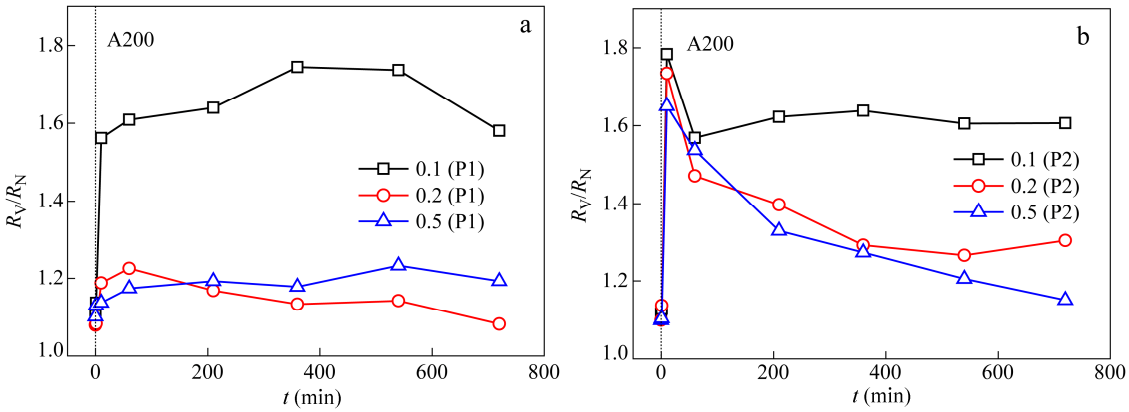


Fig. 9 R_V/R_N for the A200 silica filled (10/90 wt%) PDMS/PBD blends as a function of time after a step down of the shear rate from 30 s^{-1} to 0.1 s^{-1}: (a) with blending procedure 1 and (b) with blending procedure 2 (The numbers in the legend refer to particle concentrations (in wt%).)

The above results indicated that the time evolution of the droplet size distribution for the filled blends during coalescence is closely related to the efficiency of the nanoparticles in suppressing coalescence. For the silica nanoparticles (hydrophobic and hydrophilic), when incorporating them into the blends with procedure 1, coalescence of the dispersed PDMS phase can be suppressed efficiently by nanoparticles, causing that the polydispersity of the droplet size fluctuates narrowly and the droplet size distributions are unimodal during coalescence; while incorporating them into the blends with procedure 2, coalescence of the dispersed PDMS phase cannot be suppressed efficiently by nanoparticles, consequently R_V/R_N passes a maximum in the early stage of coalescence when the bimodal droplet size distributions occur. From the above results of the same silica nanoparticles by two different blending procedures, we can conclude that, the two different blending procedures can cause differed localization of the nanoparticles and thus affect the efficiency of the nanoparticles in suppressing coalescence, therefore leading to the droplet size distribution diverse.

Localization of Particles in the PDMS/PBD Blend

To further understand how blending procedure influences the droplet size distribution, in this section we discuss the localization of the nanoparticles in the PDMS/PBD blend. At thermodynamic equilibrium, the localization of the silica particles is governed by the affinity between nanoparticles and components through the interfacial energy. In other words, if kinetic effects do not interfere, the difference between interfacial tensions controls the

place where the silica will be localized after stopping the mixing. Two situations can be distinguished: (1) the nanoparticles are mainly distributed homogeneously within one of the two phases of polymer blends and (2) the nanoparticles are confined at the interface between the two polymers. This can be predicted qualitatively by using a wetting parameter ω, defined as follows:

$$\omega_1 = \frac{\sigma_{\text{si-2}} - \sigma_{\text{si-1}}}{\sigma_{12}} \tag{4}$$

where $\sigma_{\text{si-i}}$ is the interfacial tension between the nanoparticle and the polymer i; σ_{12} is the interfacial tension between two polymers.

When $\omega_1 > 1$, the nanoparticles are expected to be in polymer 1, and for value $\omega_1 < -1$ in polymer 2. For intermediate values of $-1 < \omega_1 < 1$, the particles are expected to be located at the interface between the two polymers.

Estimation of the interfacial tension between two components 1 and 2 can be achieved using the well-known Owens and Wendt[33] equation:

$$\sigma_{12} = \sigma_1 + \sigma_2 - 2\sqrt{\sigma_1^d \sigma_2^d} - 2\sqrt{\sigma_1^p \sigma_2^p} \tag{5}$$

where the exponents *d* and *p* stand for, respectively, the dispersive and the polar contributions to the surface tension. These values have been reported for PDMS[34], PBD[35], R972 and A200 nanosilica[28], which are given in Table 4.

Table 4. Surface tension data of the components of the blends at 25 °C

Components	σ (mN/m)	σ^d (mN/m)	σ^p (mN/m)
PDMS	19.2	18.4	0.8
PBD	32	23.8	8.2
R972	32	30	2
A200	80	29.4	50.6

For the present systems at 25 °C, according to eqs. (4) and (5), the calculated ω_{PDMS} is 0.198 for the hydrophobic R972 nanoparticles and −5.14 for the hydrophilic A200 nanoparticles. Therefore, at thermodynamic equilibrium, the hydrophilic A200 silica particles should be preferentially located in the PBD phase while the hydrophobic R972 silica particles should be found at the interface and also in PDMS. It should be noted that in molten polymers, the thermodynamic equilibrium may be difficult to reach and the kinetic effects may dominate if the viscosity is high and/or the processing time is short.

Indeed, the observed differences of the results shown in Tables 2 and 3 between the filled blends with blending procedure 1 and 2 suggest that the "initial" localization of the particles in those blends is differed. By "initial" localization we mean the one that can be observed before coalescence. If we go back to the aspect of the time evolution of the droplet size distribution, we can find that it does not depend much on the nature of the silica, but on blending procedure. This can be explained by the fact that the effect of particles on the blend is greatly affected by their localization in the blend. The localization of particles is determined by the nature of the particle (hydrophilicity or hydrophobicity) when the thermodynamic equilibrium is reached. In our study, the results have indicated that thermodynamic equilibrium is difficult to reach due to the high viscosity of the polymers. On the other hand, the mixing condition greatly affects the initial localization of particles. Because of the difficulty in reaching thermodynamic equilibrium for polymer system with high viscosity, the mixing condition becomes the key factor to influence the localization of particles. The distinct morphology evolution in the silica filled (10/90 wt%) PDMS/PBD blends prepared with different blending procedures should be ascribed to the differed "initial" localization of the particles, which can be demonstrated schematically in Fig. 10.

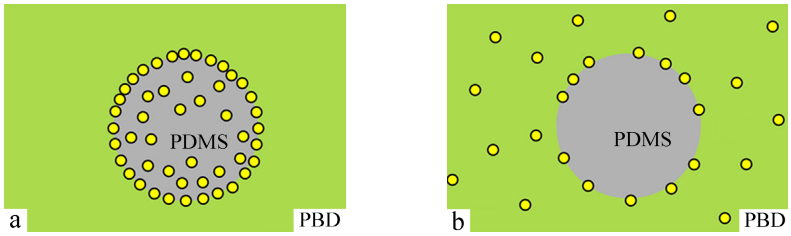


Fig. 10 Schematics of the initial location of nanoparticles in the silica filled (10/90 wt%) PDMS/PBD blends prepared with different blending procedures: (a) blends prepared with blending procedure 1 having nanoparticles mainly located at the interface between two polymers and in the PDMS phase and (b) blends prepared with blending procedure 2 having nanoparticles mainly located in the PBD phase

For the R972 silica filled blends prepared with blending procedure 1, the nanoparticles should be mainly located at the interface and in the PDMS dispersed phase and form an dense particle layer at the interface, as demonstrated schematically in Fig. 10(a). This leads to an efficient steric barrier against coalescence of the PDMS droplets (see Fig. 6). Therefore, the change in droplet size R_V is small during coalescence and the droplet size distributions are always unimodal. For the R972 silica filled blends prepared with blending procedure 2, the nanoparticles should be mainly distributed in the PBD matrix phase and the PDMS droplets are barely covered with the nanoparticles, as shown in Fig. 10(b). And this leads to an inefficient steric barrier against coalescence of the PDMS droplets (see Fig. 6). In this way, the morphology evolution in R972 filled blends is similar as that in pure (10/90 wt%) PDMS/PBD blend and thus bimodal droplet size distributions during the early coalescence occur in these filled blends.

In the same way, for the A200 silica filled blends prepared with blending procedure 2, the nanoparticles should also be mainly located in the PBD phase, as illustrated in Fig. 10(b). This leads to an poor efficient steric barrier against coalescence of the PDMS droplets (see Fig. 8) and therefore bimodal droplet size distributions can be observed, which is similar to that occur in pure (10/90 wt%) PDMS/PBD blend. For the A200 silica filled blends prepared with blending procedure 1, the nanoparticles should be mainly kinetically trapped at the interface and in the PDMS phase, as demonstrated schematically in Fig. 10(a). And this leads to an efficient steric barrier against coalescence of the PDMS droplets (see Fig. 6) and thus the droplet size distributions during coalescence are always unimodal except for the 0.1 wt% A200 filled system. The reason why the bimodal droplet size distributions occur for low concentration of A200 silica system should be attributed to the low particle content at the interface, where some originally located silica particles moved to PBD phase during coalescence because of the affinity between A200 silica particles and the PBD phase. Finally, it should be mentioned that the concentration of particles is low and we did not see any network-like structures in the present work. We believe that if the concentration of particles is high enough to cover the surface of the small droplets (produced by preshearing), coalescence of droplets should be completely suppressed; then the mean size of droplets should almost remain unchanged and the droplet size distributions should show unimodality during coalescence.

CONCLUSIONS

In the present work, the effect of silica nanoparticles on the temporal morphology of (10/90 wt%) PDMS/PBD blends during the shear induced coalescence of the droplets of the minor phase at low shear rate was investigated systematically. It has been shown that the time evolution of the drop size distribution does not depend much on the nature of the silica, but mainly on blending protocol. With the blending procedure consisting in pre-blending silica particles in PBD matrix phase, bimodal droplet size distribution occurs during the early stages of coalescence; while with the blending procedure consisting in pre-blending silica particles in PDMS disperse phase, the droplet size distribution are always unimodal during coalescence. This observation can be explained by the localization of the particles, which can be greatly affected by blending method. When the silica particles were initially mixed with PBD matrix phase, the nanoparticles should be mainly located in

the PBD phase and this leads to an inefficient steric barrier against coalescence of PDMS droplets. In this way, the morphology evolution in the filled blends is similar to that in pure (10/90 wt%) PDMS/PBD blend and thus bimodal droplet size distribution occurs during the early coalescence; while initially blending the silica particles with PDMS dispersed phase, the nanoparticles should be mainly kinetically trapped at the interface and in the PDMS phase and can provide an efficient steric barrier against coalescence of PDMS droplets. In this way, the change of the droplet size is small and the droplet size distributions tend to be unimodal during coalescence. Our results imply that control over blending procedure which exploits nonequilibrium processes allows the temporal morphology to be regulated during coalescence.

REFERENCES

1 Aveyard, R., Clint, J.H., Nees, D. and Paunov, V.N., Langmuir, 2000, 16(4): 1969
2 Binks, B.P. and Lumsdon, S.O., Langmuir, 2001, 17(15): 4540
3 Ramsden, W., Proc. R. Soc. London, A, 1903, 72(479): 156
4 Pickering, S.U., J. Chem. Soc., Trans., 1907, 91: 2001
5 Binks, B.P., Adv. Mater., 2002, 14(24): 1824
6 Binks, B.P., Dyab, A.K.F. and Fletcher, P.D.I., Chem. Commun., 2003, (20): 2540
7 Binks, B.P. and Rodrigues, J.A., Langmuir, 2007, 23(14): 7436
8 Binks, B.P. and Whitby, C.P., Langmuir, 2004, 20(4): 1130
9 Binks, B.P. and Whitby, C.P., Colloids Surf. A, 2005, 253(1–3): 105
10 Tambe, D.E. and Sharma, M.M., J. Colloid Interface Sci., 1993, 157(1): 244
11 Tambe, D.E. and Sharma, M.M., J. Colloid Interface Sci., 1994, 162(1): 1
12 Tambe, D., Paulis, J. and Sharma, M.M., J. Colloid Interface Sci., 1995, 171(2): 463
13 Vignati, E., Piazza, R. and Lockhart, T.P., Langmuir, 2003, 19(17): 6650
14 Maiti, S., De, S.K. and Bhowmick, A.K., Rubber Chem. Technol., 1992, 65(2): 293
15 Gubbels, F., Jerome, R., Vanlathem, E., Deltour, R., Blacher, S. and Brouers, F., Chem. Mater., 1998, 10(5): 1227
16 Huang, J.C., Wu, C.L. and Grossman, S.J., J. Polym. Eng., 2000, 20(3): 213
17 Clarke, J., Clarke, B., Freakley, P.K. and Sutherland, I., Plast. Rubber Compos., 2001, 30(1):39
18 Ibarra-Gomez, R., Marquez, A., Valle, L.F.R.D. and Rodriguez-Fernandez, O.S., Rubber Chem. Technol., 2003, 76(4): 969
19 Ray, S.S., Pouliot, S., Bousmina, M. and Utracki, L.A., Polymer, 2004, 45(25): 8403
20 Ray, S.S. and Bousmina, M., Macromol. Rapid Commun., 2005, 26(20): 1639
21 Austin, J.R. and Kontopoulou, M., Polym. Eng. Sci., 2006, 46(11): 1491
22 Si, M., Araki, T., Ade, H., Kilcoyne, A.L.D., Fisher, R., Sokolov, J.C. and Rafailovich, M.H., Macromolecules, 2006, 39(14): 4793
23 Hong, J.S., Namkung, H., Ahn, K.H., Lee, S.J. and Kim, C., Polymer, 2006, 47(11): 3967
24 Hong, J.S., Kim, Y.K., Ahn, K.H., Lee, S.J. and Kim, C., Rheol. Acta, 2007, 46(4): 469
25 Vermant, J., Cioccolo, G., Nair, K.G. and Moldenaers, P., Rheol. Acta, 2004, 43(5): 529
26 Vandebril, S., Vermant, J. and Moldenaers, P., Soft Matter, 2010, 6(14): 3353
27 Thareja, P. and Velankar, S., Rheol. Acta, 2007, 46(3): 405
28 Elias, L., Fenouillot, F., Majeste, J.C. and Cassagnau, P., Polymer, 2007, 48(20): 6029
29 Tong, W., Huang, Y.J., Liu, C.L., Chen, X.L., Yang, Q. and Li, G.X., Colloid Polym. Sci., 2010, 288(7): 753
30 Elias, L., Fenouillot, F., Majeste, J.C., Martin, G. and Cassagnau, P., J. Polym. Sci. Part B: Polym. Phys., 2008, 46(18): 1976
31 Anastasiadis, S.H., Chen, J.K., Koberstein, J.T., Sohn, J.E. and Emerson, J.A., Polym. Eng. Sci., 1986, 26(20): 1410
32 Ziegler, V.E. and Wolf, B.A., Polymer, 2005, 46(22): 9265
33 Owens, D.K. and Wendt, R.C., J. Appl. Polym. Sci., 1969, 13(8): 1741
34 Thareja, P. and Velankar, S.S., Colloid Polym. Sci., 2008, 286(11): 1257
35 Lee, L.H., J. Polym. Sci. Part B: Polym. Phys., 1967, 5(6): 1103